Clean Techn Environ Policy (2017) 19:77–91
DOI 10.1007/s10098-016-1190-3

ORIGINAL PAPER

Energy efficiency of RO and FO–RO system for high-salinity seawater treatment

Ali Altaee[1] · Graeme J. Millar[2] · Guillermo Zaragoza[3] · Adel Sharif[4]

Received: 20 January 2016 / Accepted: 15 April 2016 / Published online: 26 April 2016

Abstract Forward osmosis (FO) has been proposed as an alternative method for seawater desalination, wherein reverse osmosis (RO) membrane technology is used for regeneration of the draw solution. Previous studies have indicated that a standalone RO unit is more energy efficient than an FO–RO system, and as such it was recommended that an FO–RO system is best employed only for the desalination of high-salinity seawaters. This study examined FO–RO applicability in more detail by examining the impact of seawater salinity, impact of an energy recovery device (ERD), and the effect of membrane fouling. For comparison purposes, the performance of the FO process was improved to minimize the impact of concentration polarization and optimize the concentration of draw solution. Model calculations revealed that FO–RO is more energy efficient than RO when no ERD was employed. However, results showed that there was no significant difference in the power consumption between the FO–RO system and the RO unit at high seawater salinities particularly when a high-efficiency ERD was installed. Moreover, the FO–RO system required more membrane area than a conventional RO unit which may further compromise the FO–RO desalination cost.

✉ Ali Altaee
alialtaee@hotmail.com

[1] AquaMa Ltd, 31 Old Palace Road, Guildford, Surrey GU2 7TU, UK

[2] Science and Engineering Faculty, Institute for Future Environments, Queensland University of Technology (QUT), Brisbane, QLD 4000, Australia

[3] CIEMAT, Plataforma Solar de Almería, Ctra. de Senés s/n, 04200 Tabernas, Almería, Spain

[4] QEERI, HBKU, Qatar Foundation, Doha, Qatar

Introduction

Water scarcity is a growing problem which heightens the concerns of water supply to major cities in the long-term perspective (Jiang 2015). Factors such as groundwater pollution, climate change, and population growth have combined to increase the demand for drinking water (Maxwell 2010). Several methods have been suggested to counter the problem of water shortage including wastewater reuse (Gude 2016) and seawater desalination (Bennett 2015). Despite wastewater reuse being cheaper than desalination, there are many barriers preventing its widespread application for human use (Salgot 2008). Seawater desalination is now the most common method for freshwater supply into cities in arid and semi-arid regions (Youssef et al. 2014). However, there is increasing concern on the effect that the fast development of desalination may have on the environment. Desalination is an energy-intensive process and can turn the water problem into an energy problem (Gilron 2014). The use of renewable energy sources can mitigate the energy impact on sustainability (Cipollina et al. 2015), but there is still the need to improve energy efficiency of desalination (Horta et al. 2015).

Commercial desalination technologies are divided into thermal and membrane processes; thermal approaches include multi-stage flash (MSF) and multi-effect distillation (MED) (Bataineh 2016), whereas reverse osmosis (RO) is the main membrane technology for seawater desalination (Rodríguez-Calvo et al. 2015). MSF and MED processes have been extensively employed for seawater desalination, particularly in the Middle East, and are capable of producing very high-quality water (Mezher et al. 2011). However, thermal technologies require relatively high energy consumption, despite advances such as

integration of MED and thermal vapour compression (Al-Mutaz and Wazeer 2015). Membrane technology is generally more energy efficient than thermal processes. For example, RO typically requires 3.37 kW h/m^3 of energy for desalinating seawater, 1.2 kW h/m^3 for industrial effluent, and 0.7–1 kW h/m^3 for brackish water (Hoang et al. 2009). Modern seawater desalination plants incorporating RO usually employ an energy recovery device (ERD). Previous studies (Mamo et al. 2013) reported that energy consumption was reduced to <2.0 kW h/m^3 for a range of commercially available RO membranes when tested with water from the Pacific Ocean and with a unit containing an ERD. However, RO processes normally require an intensive pretreatment strategy for the removal of fouling materials from the feed water (Sun et al. 2015). Fouling problems adversely impact the performance of RO membrane and increase the energy requirements for desalination (Kim et al. 2015).

Forward osmosis (FO) has been proposed as an alternative technology for the sustainable supply of clean water (Su et al. 2012). Its potential as a sustainable technology for desalination has been explored for different applications in the water industry (Nasr and Sewilam 2015), including treatment of oil sands produced water (Bhinder et al. 2016), processing of saline wastewater (Roy et al. 2016), and even for irrigation through fertilizer-drawn FO (Majeed et al. 2015). The most important use, however, is seawater desalination (Webley 2015), wherein it can be employed either as a pretreatment stage to protect downstream RO modules (Qin et al. 2009) or as the central desalination step (Mazlan et al. 2016). FO processes have been suggested to be less energy intensive and of lower environmental impact than conventional desalination processes; hence, this technique has received a lot of attention by researchers and scientists as an alternative to the RO process. FO utilizes the natural osmosis phenomenon for freshwater extraction from seawater using a concentrated salt solution as the draw agent (Valladares et al. 2014). Current state of the art regarding FO research is focused on membrane development (Sato and Nakao 2016), optimization of the draw solution (Zhao et al. 2016), and the use of hybrid systems (Chekli et al. 2016). This work is focused on the latter aspect, arising as a result of the necessity to use a second stage in FO to separate the draw agent from the freshwater (Luo et al. 2014). RO is one of the technologies proposed for the regeneration and reuse of the draw agent (Shaffer et al. 2015). The regenerated draw solution is recycled to the FO membrane to reduce the overall chemical cost (Fig. 1). Analysis by McGovern and Lienhard (2014) suggested that RO was more energetically favourable for seawater desalination than a comparable FO system due to the significant energy demand of the draw solution regeneration step. The study recommended that an FO–RO system should be most applicable for high-salinity feed waters where RO is less competitive. Shaffer et al. (2015) also described similar findings and emphasized that a hybrid FO–RO process may be best suited to water which cannot easily be treated by RO due to for example high salinity and/or high potential for membrane fouling. Mazlan et al. (2016) suggested that any advantages of the combined FO–RO system were related not to energy reduction but to reduction in pretreatment costs prior to an RO unit or a decrease in chemical cleaning requirements due to diminished fouling of the RO membrane.

Our previous work generally agreed with other authors and concluded that FO–RO is more suitable for high-salinity seawater (Altaee et al. 2014). However, the latter study did not take into account the impact of membrane fouling on the process performance and power consumption, which resulted in underestimation of the energy requirements for the desalination. Ignoring the role of an ERD has inhibited the accurate prediction of the desalination energy requirements. Subsequent studies (McGovern and Lienhard 2014) incorporated an ERD in the calculations of power consumption but did not include the impact of seawater salinity on the power consumption. The outlined study also overlooked the impact of RO membrane fouling. Furthermore, an FO process needs to be optimized before the performance is carried out with the state-of the-art RO process. As such, the previous impression that FO process would assist in reducing the power consumption of desalination may be exaggerated and there is no study as yet, which provides detailed information about the performance of an FO–RO system in comparison with RO process. The investigation presented in this paper focused on understanding the impact upon energy efficiency of conventional RO and FO–RO systems, with and without an ERD, when taking into account performance deterioration of the RO membrane over time. Since ERD may not be installed in some small-scale RO plants because of the initial high capital and installation costs, it was necessary to consider plants with or without this latter feature (Gude 2011). It should be noted that RO process has been in the market for a relatively long time and the state-of-the-art and key operating parameters are well understood. For comparison purposes, the performance of the FO process was optimized to reduce the operating cost of the FO–RO system. Key parameters such as FO feed flow rate, membrane area, and membrane flux of the FO process were optimized to reduce the effect of concentration polarization (CP) on the membrane performance using a pre-developed computer model. The model also estimated the required concentration of draw solution for seawater desalination, which would reduce the cost of regeneration by the RO process.

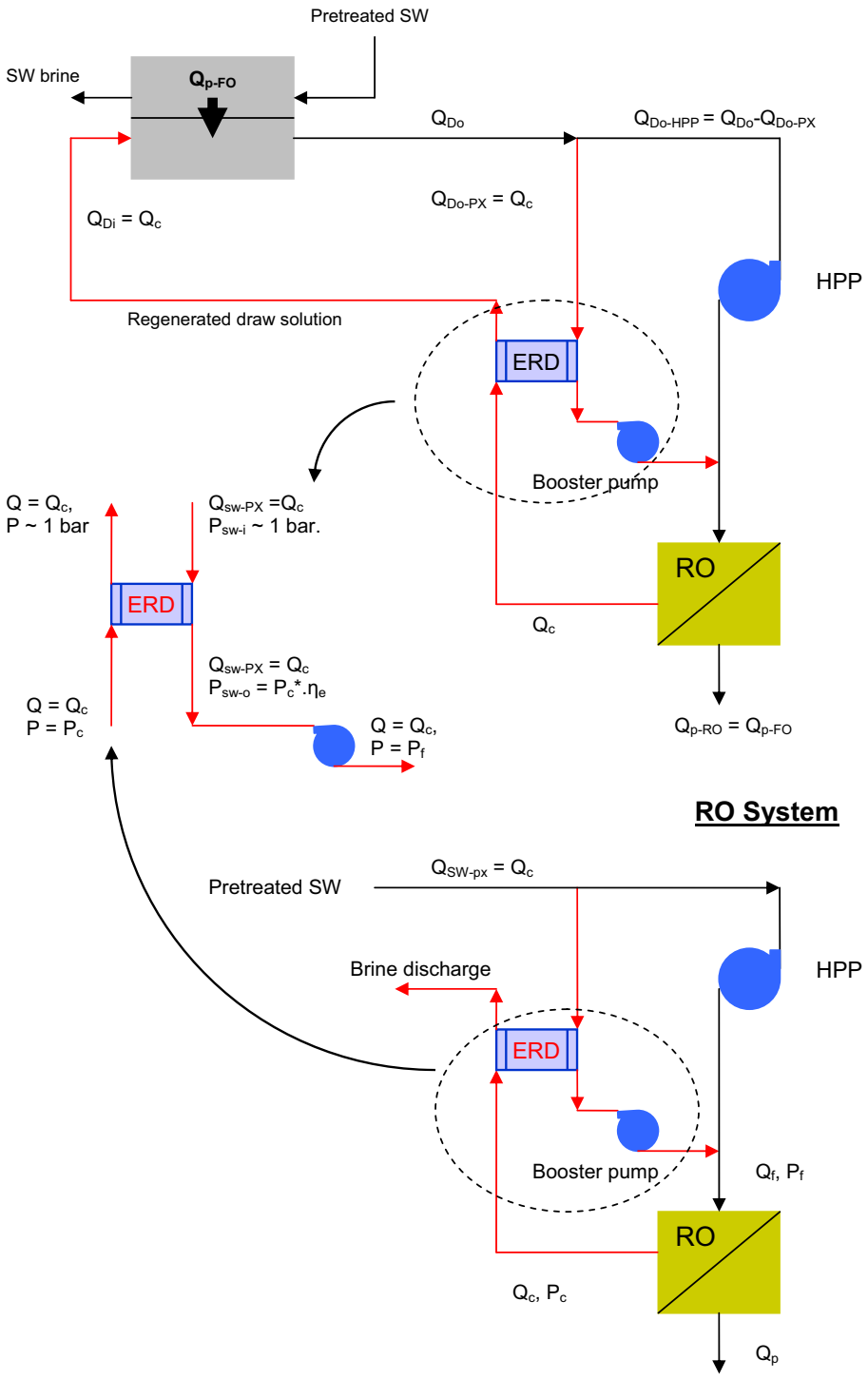

Fig. 1 Schematic diagram of FO–RO system (energy recovery device, ERD)

Reverse osmosis performance

RO processes have been used for seawater desalination for more than three decades (Chung et al. 2015); the process performance and operating parameters are well understood and optimized (Patroklou and Mujtaba 2014). Water flux, J_w (L/m^2 h), in the RO membrane system is usually estimated from Eq. 1:

$$J_w = A_w(\Delta P - \mathrm{CP} \times \Delta\pi_{Fb}), \quad (1)$$

where A_w is the water permeability coefficient (L/m^2 h bar), ΔP is the pressure gradient across the membrane (bar), CP is the CP factor, and $\Delta\pi_{Fb}$ is the osmotic pressure gradient across the membrane. In fact, J_w represents water flux over a clean RO membrane, hence it was essential to account for membrane fouling in the RO process before evaluating the

performance of the conventional RO and FO–RO systems. Fouling is an inevitable phenomenon in the RO filtration process and results in a decline of water flux over time. This latter behaviour can be approximated as an annual membrane flux decline between 7 and 10 % (Hydranautics Design Limits 2015) in the conventional RO system, where the typical silt density index (SDI) of feed water is <5 (Iwahori et al. 2003). For the RO step in the FO–RO system, feed water SDI <1, the annual decline of membrane flux is approximated between 2 and 4 % (McGovern and Lienhard 2014). In the current study, the annual flux decline in conventional standalone RO and the RO step in the FO–RO system was assumed to be 8 and 3 %, respectively. Mathematically, water flux in year n for the fouled RO membrane was equal to the initial membrane flux minus annual water flux decline in the membrane as described in Eq. 2:

$$J_n = J_0 - (Y_n \cdot J_0), \tag{2}$$

where J_n is the permeate flux in year n (L/m^2/h), J_0 is the initial permeate flux, n is the number of years, and Y is the annual percentage of flux decline. The second term on the right-hand side of Eq. 2 represented annual flux decline in the fouled RO membrane. As such, permeate flow rate in the year n, Q_{pn}, was equal to the J_n multiplied by the membrane area, A (m^2) (Eq. 3):

$$Q_{pn} = J_n \times A. \tag{3}$$

As mentioned before, Y values for the conventional RO system and RO step in the FO–RO system were assumed to be 8 and 3 %, respectively (Hydranautics Design Limits 2015). Flux decline affected the specific power consumption of the RO process, E_s (kW h/m^3), which was estimated from Eq. 4:

$$E_s = \frac{P_f \times Q_f}{\eta \times Q_p}. \tag{4}$$

In Eq. 4, P_f is the feed pressure (bar), Q_f is the feed flow rate (m^3/h), η is the pump efficiency (it is assumed 0.8 here), and Q_p is the permeate flow rate (m^3/h). If the RO process operated at fixed P_f, the permeate flow rate decreased over time due to membrane fouling. Eventually, this behaviour increased the specific power consumption of the RO process; the annual increase in specific power consumption, E_{sn} (kW h/m^3), was estimated from Eq. 5:

$$E_{sn} = \frac{P_f \times Q_f}{\eta \times J_n \times A}, \tag{5}$$

where A is the membrane area (m^2). Equation 5 can be used to estimate the specific power consumption of the RO process without ERD which was likely to happen in some smaller capacity desalination plants (Bates et al. 2015).

For both the RO and FO–RO systems, model calculations were carried out for 8 in. diameter Dow FILMTEC SW30HRLE-400i RO membrane, assuming that each pressure vessel contained eight RO modules (AlTaee and Sharif 2011). Most of the commercially available RO membranes have a rejection rate >99 % to monovalent ions (Mamo et al. 2013); for example, the rejection rate of Dow FILMTEC SW30HRLE-400i membrane to NaCl was about 99.75 %. There were a number of assumptions made in the current study to simplify the evaluation of RO and FO module performance in both the conventional RO and the FO–RO systems:

1. The decline in the annual membrane flux, J_n, was assumed to be 8 % per year for the conventional RO system and 3 % for the RO step in the FO–RO system. It was considered that flux decline in the RO step of the FO–RO system was equal to that of the second pass of dual-pass RO process (McGovern and Lienhard 2014).
2. Feed pressure, P_f, was assumed to be constant over the membrane life. This implied that both membrane flux and recovery rate decreased with membrane age. It should be mentioned that in a real RO system, P_f would be increased to maintain the desired flux and recovery rate as the membrane fouled.
3. The life of RO membrane was assumed to be 5 years for both the conventional RO system and the RO step in the FO–RO system (Bates et al. 2015). However, the life of the RO step in the FO–RO system may exceed 5 years due to the lower membrane fouling propensity.
4. SDI in the conventional RO process was <5 assuming an open intake system feed water, whereas the SDI of the RO step in the FO–RO system was <1 or RO permeate feed water.

RO system analysis version 9.1 (ROSA 9.1) software was applied to estimate the initial performance of the conventional RO system and the RO step in the FO–RO system. Feed water to a conventional RO system had a higher SDI than the RO step in the FO–RO system; the higher the SDI of feed water, the higher the membrane fouling propensity was (Rachman et al. 2013). Typically, higher feed flow rates are recommended to reduce membrane fouling at higher feed SDI (Altaee et al. 2014).

RO plant with ERD

For most large capacity RO desalination plants, an ERD is installed for energy recovery from the concentrated RO brine before discharge. This energy is exchanged with part of the seawater feed to the RO system (Dimitriou et al. 2015) (Fig. 2). In the current study, ERD with 80 and 98 % efficiency was evaluated for energy recovery from the RO brine (Peñate and García-Rodríguez 2011). In general, the energy recovered by the ERD, W_{ERD}, was a function of the

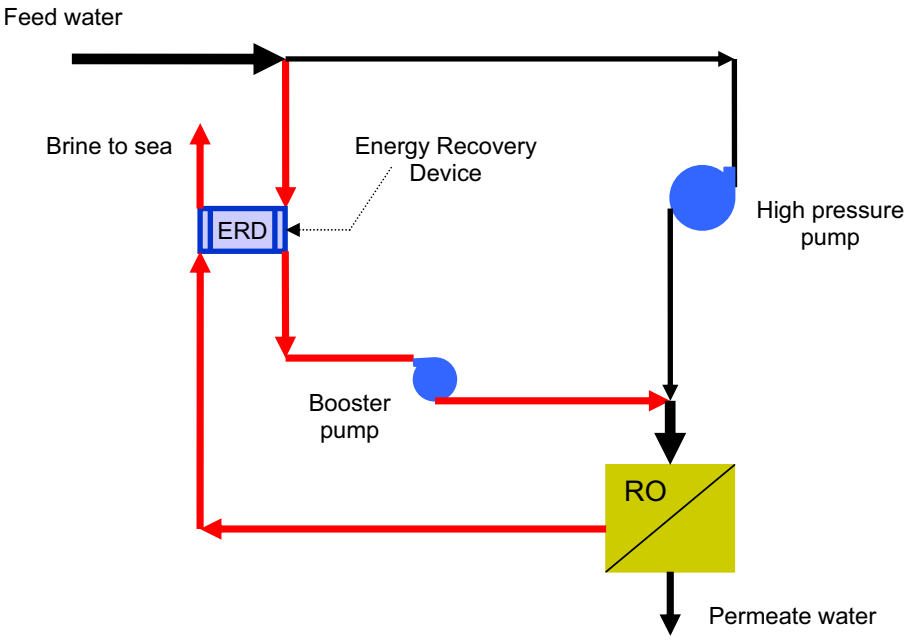

Fig. 2 RO system with energy recovery device (RED)

RO brine pressure, flow rate, and the ERD efficiency as shown in Eq. 6 (Stover 2007):

$$W_{\mathrm{ERD}} = P_{\mathrm{c}} \times Q_{\mathrm{c}} \times \eta_{\mathrm{ERD}}, \tag{6}$$

where η_{ERD} is the efficiency of the ERD, P_{c} is the pressure of RO brine (bar), and Q_{c} is the flow rate of the RO brine (m^3/h). Practically, W_{ERD} energy is exchanged with the part of seawater feed going to the ERD (Fig. 2); substituting in Eq. 6 gives Eq. 7:

$$P_{\mathrm{swo}} \times Q_{\mathrm{sw}} = P_{\mathrm{c}} \times Q_{\mathrm{c}} \times \eta_{\mathrm{ERD}}, \tag{7}$$

where P_{swo} is the outlet pressure of seawater leaving the ERD (bar) and Q_{sw} is the seawater flow rate to the ERD (m^3/h). Ignoring leakage losses, the volumetric flow rate of RO brine, Q_{c}, in Eq. 7 was equal to that of the seawater, Q_{sw} (Eq. 8):

$$P_{\mathrm{swo}} = P_{\mathrm{c}} \times \eta_{\mathrm{ERD}}. \tag{8}$$

Equation 8 shows that the feed pressure of seawater leaving the ERD was a function of the RO brine pressure and the efficiency of the ERD. It should also be mentioned that P_{swo} was equal to the inlet pressure of the booster pump. The specific energy, E_{s} (kW h/m^3), required to desalinate seawater by RO system was estimated from Eq. 9 (Stover 2007):

$$E_{\mathrm{s}} = \frac{(W_{\mathrm{HPP}} + W_{\mathrm{BP}} + W_{\mathrm{SP}})}{Q_{\mathrm{p}}}, \tag{9}$$

where W_{HPP} is the energy consumed by the high-pressure pump (kW), W_{BP} is the energy consumed by the booster pump (kW), W_{SP} is the energy consumed by the supply pump (kW), and Q_{p} is the permeate flow rate (m^3/h). In terms of feed pressure and flow rate, the specific energy required for seawater filtration by the RO membrane can be expressed as shown in Eq. 10 (Valladares et al. 2014):

$$E_{\mathrm{s}} = \frac{\frac{Q_{\mathrm{HPP}}(P_{\mathrm{HPP}} - P_{\mathrm{F}})}{\eta_{\mathrm{HPP}}} + \frac{Q_{\mathrm{BP}}(P_{\mathrm{HPP}} - P_{\mathrm{BPin}})}{\eta_{\mathrm{BP}}} + \frac{Q_{\mathrm{SP}} \times P_{\mathrm{F}}}{\eta_{\mathrm{SP}}}}{Q_{\mathrm{p}}}, \tag{10}$$

where Q_{HPP}, Q_{BP}, and Q_{SP} are the feed flow rates to the high-pressure pump, booster pump, and supply pump, respectively (m^3/h); η_{HPP}, η_{BP}, and η_{SP} are the high-pressure pump, booster pump, and supply pump efficiencies, respectively, P_{HPP} is the high-pressure pump outlet pressure (bar), P_{BPin} is the booster pump inlet pressure (bar), and P_{F} is the pressure of feed flow (bar). Equation 10 can be used to estimate the specific power consumption of the RO process with the ERD. The first and second terms on the right-hand side of Eq. 10 expressed the specific power consumed for seawater filtration by the RO membrane, while the third term on the right-hand side expressed power requirement for seawater pumping to the RO system. To include flux decline due to fouling, permeate flow in year n, $Q_{\mathrm{p}n}$, replaced the Q_{p} term in Eq. 10 as illustrated in Eq. 11:

$$E_{\mathrm{s}} = \frac{\frac{Q_{\mathrm{HPP}}(P_{\mathrm{HPP}} - P_{\mathrm{F}})}{\eta_{\mathrm{HPP}}} + \frac{Q_{\mathrm{BP}}(P_{\mathrm{HPP}} - P_{\mathrm{BPin}})}{\eta_{\mathrm{BP}}} + \frac{Q_{\mathrm{SP}} \times P_{\mathrm{F}}}{\eta_{\mathrm{SP}}}}{Q_{\mathrm{pn}}}. \tag{11}$$

FO process performance and optimization

The recovery rates in the FO and RO processes of the FO–RO system were equal (Fig. 1). Freshwater permeated across the FO membrane from the feed solution and diluted the draw solution. The diluted draw solution split into two flows after leaving the FO membrane (Fig. 1); the first flow

went to an ERD to exchange pressure with the RO brine, Q_c (the regenerated draw solution). The second flow went to a high-pressure pump for pressurization before the RO treatment. The RO permeate was the product water, whereas the concentrate was the regenerated draw solution to be reused in the FO process. Water flux, J_w (L/m^2 h), in the ideal FO process, with reflection coefficient equal to one and insignificant CP effects can be calculated from Eq. 12:

$$J_w = A_w(\pi_{Db} - \pi_{Fb}), \tag{12}$$

where A_w is the water permeability coefficient (L m^2 h bar), π_{db} is the osmotic pressure of bulk draw solution (bar), and π_{Fb} is the osmotic pressure of bulk feed solution (bar). Theoretical water flux in the FO process was higher than experimental water flux due to the phenomenon of CP at the membrane–solution interface. The expression usually used to estimate water flux in an FO process when draw solution faces the membrane active layer (DS-AL) is shown in Eq. 13 (Tiraferri et al. 2013):

$$J_w = A_w\left(\frac{\pi_{Db}e^{\left(\frac{-J_w}{k}\right)} - \pi_{Fb}e^{(J_wK)}}{1 + \frac{B}{J_w}\left(e^{(J_wK)} - e^{\left(\frac{-J_w}{k}\right)}\right)}\right), \tag{13}$$

where k is the bulk mass transfer coefficient (m/s), B is the solute permeability coefficient (m/h), and K is the solute resistivity for diffusion within the porous support layer (s/m). The negative exponential term represented the dilutive CP effect on the draw solution side; it was indicative of the lower concentration at the membrane surface than in the bulk solution. Simultaneously, concentrative CP occurred at the feed solution side and it was represented by the positive exponent which indicated a higher concentration at the membrane surface than in the bulk solution. Water flux in Eq. 13 approached that in Eq. 12 when the permeate flux was very low. In previous studies, FO optimization was not performed in the comparison studies between the conventional RO and the FO–RO systems. (Altaee et al. 2014). FO optimization should reduce the cost of the RO regeneration process in the FO–RO system which was responsible for the majority of the energy consumption in the desalination process. The performance of the FO process was significantly affected by dilutive and concentrative CP at the draw and feed solution sides, respectively. Equation 13 depicts the effect of CP on the performance of FO process; the equation can be presented as Eq. 12 when the CP effect was negligible. Theoretically, this latter situation was possible at very low permeate flow at which the moduli of concentrative and dilutive CP, $e^{\frac{-J_w}{k}}$ and e^{J_wK}, respectively, were approaching unity. Mathematically, J_w can be expressed as the ratio of permeate flow to the membrane area: $J_w = Q_p/A_{FO}$. Therefore, at constant Q_p, membrane area was a key factor in determining the membrane flux, with the higher the Q_p, the lower the permeate flux was. Moreover, Eq. 13 indicates the importance of the net driving force, which was the differential osmotic pressure between the bulk concentration of the feed solution and the bulk concentration of the draw solution, on the membrane flux. The osmotic pressure of outlet feed pressure, π_{Fo}, was estimated from the inlet feed osmotic pressure, π_{Fi}, and the membrane recovery rate, Re, which was the ratio of permeate to feed flow rate. Thus, π_{Fo} was given as illustrated in Eq. 14:

$$\pi_{Fo} = \frac{\pi_{Fi}}{1 - \frac{Q_p}{Q_{Fi}}}, \tag{14}$$

where Q_p and Q_{Fi} are the permeate and inlet feed flow rates (m^3/h). The osmotic pressure of bulk feed solution, π_{Fb}, was the average of the inlet and the outlet feed osmotic pressure (Eq. 15):

$$\pi_{Fb} = \frac{\pi_{Fi} + \pi_{Fo}}{2}. \tag{15}$$

Substituting Eq. 14 in Eq. 15 gave Eq. 16:

$$\pi_{Fb} = \frac{\pi_{Fi} + \frac{\pi_{Fi} \times Q_{Fi}}{Q_{Fi} - Q_p}}{2}. \tag{16}$$

Equation 16 shows that the feed flow rate was a key factor in determining the osmotic pressure of bulk feed solution and should be taken into account in the optimization of the FO process. In the current study, FO optimization was performed based on the following:

1. *Membrane area* The moduli of dilutive and concentrative CP approached unity by reducing the permeate flux, which was achieved by increasing the membrane area.
2. *Feed flow rate* Increasing the feed flow rate increased the osmotic driving force across the FO membrane.
3. *Concentration of draw solution* The higher the concentration of the draw solution, the higher the power consumption in the RO regeneration unit.

Practically, permeate flows in the FO and RO processes were equal to maintain the FO–RO system in equilibrium. It was assumed that NaCl was the draw agent in the FO process because it was inexpensive, available and exhibited high osmotic pressure. The osmotic pressure of the outlet draw solution, π_{Do} (bar), was estimated from the Van't Hoff equation (Altaee et al. 2014) (Eq. 17):

$$\pi_{Do} = \frac{C_{Nao} \times 1.12 \times T}{M_{Na} \times 14.5} + \frac{C_{Clo} \times 1.12 \times T}{M_{Cl} \times 14.5}, \tag{17}$$

where C_{Nao} and C_{Clo} are the outlet concentrations of Na^+ and Cl^- ions, respectively, in the draw solution (mg/L), T is the draw solution temperature in Kelvin (273+ °C), and M_{Na} and M_{Cl} are the molecular weights of Na^+ and Cl^- ions, respectively (mg/

M). C_{Clo} in Eq. 17 can be expressed as the ratio of M_{Cl}–M_{Na} multiplied by C_{Nao}, i.e. $C_{Nao} = (M_{Cl}/M_{Na}) \times C_{Nao}$. Furthermore, the outlet pressure, π_{Do}, should be equal to or higher than the inlet pressure of feed solution, π_{Fi}. It was assumed here that $\pi_{Do} = \pi_{Fi} + 2$ to assure permeation flow in the direction of draw solution [noting that feed and draw solutions flow in a counter-current direction (Fig. 3)]. Since the osmotic pressure of seawater is known (π_{Fi}), the value of π_{Do} can be estimated and compensated in Eq. 17 to calculate C_{Nao} (Eq. 18):

$$\pi_{Do} = \frac{C_{Nao} \times 1.12 \times T}{M_{Na} \times 14.5} + \frac{\left(\frac{M_{Cl}}{M_{Na}}\right) \times C_{Nao} \times 1.12 \times T}{M_{Cl} \times 14.5}. \quad (18)$$

Assuming $\frac{1.12 \times T}{M_{Na} \times 14.5}$ and $\frac{\left(\frac{M_{Cl}}{M_{Na}}\right) \times 1.12 \times T}{M_{Cl} \times 14.5}$ are equal to constants $L1$ and $L2$, respectively, C_{Nao} is calculated from Eq. 19:

$$C_{Nao} = \frac{\pi_{Do}}{L1 + L2}. \quad (19)$$

The outlet concentration of Cl^-, C_{Clo}, was calculated from $C_{Clo} = (M_{Cl}/M_{Na}) \times C_{Nao}$ and the outlet concentration of NaCl draw solution, C_{Do}, was given by Eq. 20:

$$C_{Do} = \sum C_{Nao} + C_{Clo}. \quad (20)$$

The inlet concentration of the draw solution, C_{Di}, was estimated from the mass balance at the draw solution side of the FO membrane (Fig. 3):

$$C_{Di} = \frac{(C_{Do} \times Q_{Do}) - (Q_p \times C_p)}{Q_{Di}}, \quad (21)$$

where Q_{Di} and Q_{Do} are the inlet and outlet flow rates of the draw solution, respectively (m^3/h), C_{Do} is the outlet concentration of the draw solution (mg/L), C_p is the concentration of permeate (mg/L), and Q_p is the flow rate of permeate (m^3/h). C_p is estimated from Eq. 22 (Altaee and Zaragoza 2014):

$$C_p = \frac{B \times C_f}{J_w + B}. \quad (22)$$

Equation 13 is rearranged to calculate the bulk osmotic pressure of feed solution, knowing that π_{Db} is the average of π_{Do} and π_{Di}, and J_w is the ratio of Q_p–A_{FO} (Eq. 23):

$$\pi_{Fb} = \frac{\pi_{Db} \times e^{\frac{-J_w}{k}} - \left[\left(1 + \frac{B}{J_w}\left(e^{J_w K} - e^{\frac{-J_w}{k}}\right)\right) \times \frac{J_w}{A_w}\right]}{e^{J_w K}}. \quad (23)$$

From π_{Fb}, the outlet osmotic pressure of feed solution, π_{Fo}, was calculated from the expression shown in Eq. 24:

$$\pi_{Fo} = \pi_{Fb} \times 2 - \pi_{Fi}. \quad (24)$$

In Eq. 24, π_{Fi} is the osmotic pressure of the seawater to the FO membrane (bar) and π_{Fb} was calculated from Eq. 23. For FO membrane of high rejection rate, the concentration of the outlet feed concentrate, C_{Fo}, was equal to the inlet feed concentration, C_{Fi}, multiplied by the concentration factor, 1/1 − Re (Fig. 3) (Eq. 25):

$$C_{Fo} = \frac{C_{Fi}}{1 - Re}. \quad (25)$$

Rearranging Eq. 25 in terms of recovery rate, Re (%), gave Eq. 26:

$$1 - Re = \frac{C_{Fi}}{C_{Fo}}. \quad (26)$$

Assume that the ratio of inlet feed concentration to the outlet feed concentration was equal to the corresponding ratio of osmotic pressure; compensating in Eq. 26 and rearranging the expression to calculate Re, we can derive Eq. 27:

$$Re = 1 - \frac{\pi_{Fi}}{\pi_{Fo}}. \quad (27)$$

Equation 27 can be used to estimate Re (%) in the FO process. However, Re can also be expressed as the ratio of Q_p–Q_{Fo}, hence the feed flow rate was estimated from Eq. 28:

$$Q_{Fi} = \frac{Q_p}{Re}. \quad (28)$$

Equation 28 can be used to predict the inlet feed flow rate to the FO process. The suggested model to predict the area of FO membrane, feed flow rate, and the concentration of draw solution is illustrated in Fig. 4. It should be mentioned that Q_p was estimated based on the recovery rate of the RO step in the FO–RO system.

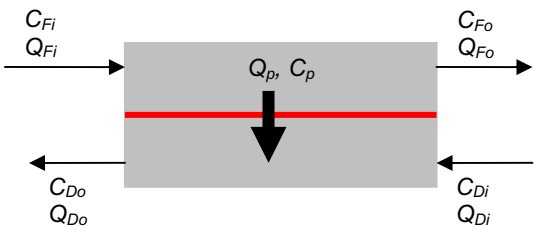

Fig. 3 Feed and draw solution mass balance in the FO membrane

FO model testing

The FO process model was validated using experimental data from literature (Achilli et al. 2009). The model parameters are listed in Table 1. The calibrated model showed good agreement with the experimental data (Table 2). In general, the difference in membrane flux was between 2.5 and 8.9 % at 35 g/L draw solution. At 60 g/L draw solution, the difference in water flux decreased between 3.5 and 8.2 % depending on feed water salinity.

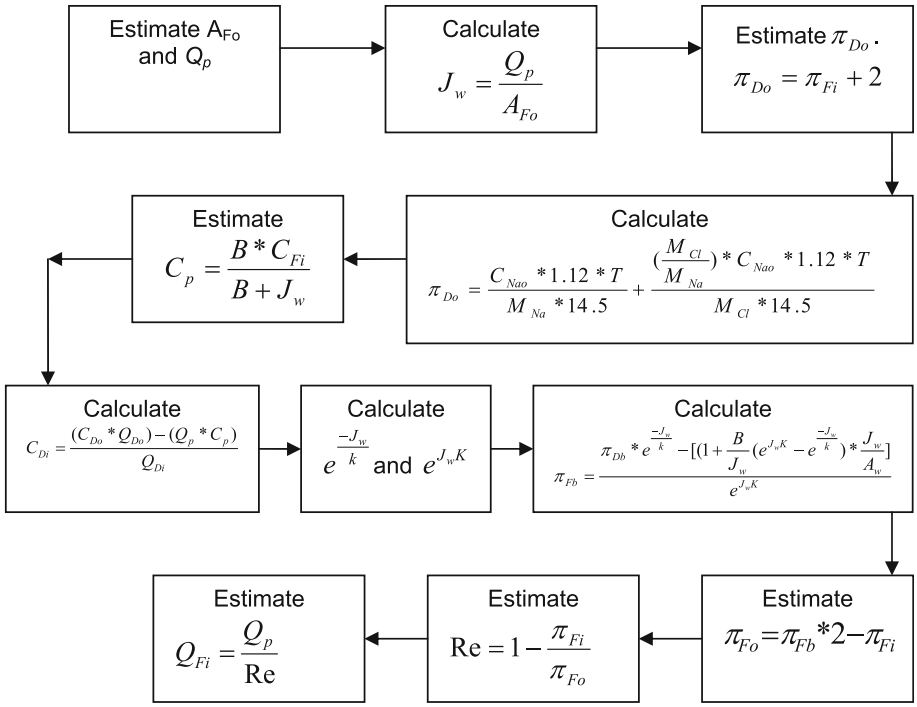

Fig. 4 FO process modelling and optimization

Table 1 Model parameters for FO simulations

Parameter	k (m/h)	S ($\times 10^{-6}$) (m)	K (h/m)	A_w ($\times 10^{-3}$) (m/h bar)	Temp. (°C)	D ($\times 10^{-6}$) (m^2/h)	B ($\times 10^{-3}$) (m/h)
Value	0.31	800	23	0.79	25	6.45	0.12

Table 2 Water flux from experimental and model tests

Draw TDS (g/L)	Feed TDS (g/L)	Pressure (bar)	$J_{w\text{-exp}}$ (L/m^2 h)	$J_{w\text{-mod}}$ (L/m^2 h)	% Diff. J_w
35	0	13	7.9	7.7	2.5
	2.5	12	6.8	6.2	8.8
	5	11	5.6	5.1	8.9
60	0	24	12.4	12	3.5
	2.5	23	10.1	9.5	5.9
	5	22.5	8.5	7.8	8.2

These results suggested that the FO model was able to satisfactorily predict water flux in the FO process.

Results and discussion

Impact of membrane area and feed flow rate on the FO performance

The impact of membrane area, A_{FO}, on the performance of the FO process was realized through reducing the effects of dilutive and concentrative CP. The concentration and osmotic pressure of the feed solution were 35 g/L and 26.2 bar, respectively. One mol (~58.5 g/L) of NaCl was used as the draw solution employed for the FO process. In the model calculations performed at 46 % feed recovery rate, A_{FO} increased from 20 to 140 m^2 and permeate flux was calculated. Moduli of dilutive and concentrative CP, $e^{\frac{-J_w}{k}}$ and $e^{J_w K}$, were calculated at different A_{FO}. As previously explained, $e^{\frac{-J_w}{k}}$ and $e^{J_w K}$ values close to unity were indicative of insignificant CP effect. Simulation results showed that $e^{\frac{-J_w}{k}}$ and $e^{J_w K}$ values approached unity with increasing A_{FO} (Fig. 5a); this latter behaviour was attributed to the low permeate flux (Fig. 5b). At 20 m^2, $e^{\frac{-J_w}{k}}$ and $e^{J_w K}$ were 0.928 and 1.7, respectively, indicating a relatively high CP effect but changed to 0.99 and 1.08 at 140 m^2. The corresponding J_w values at 20 and 140 m^2

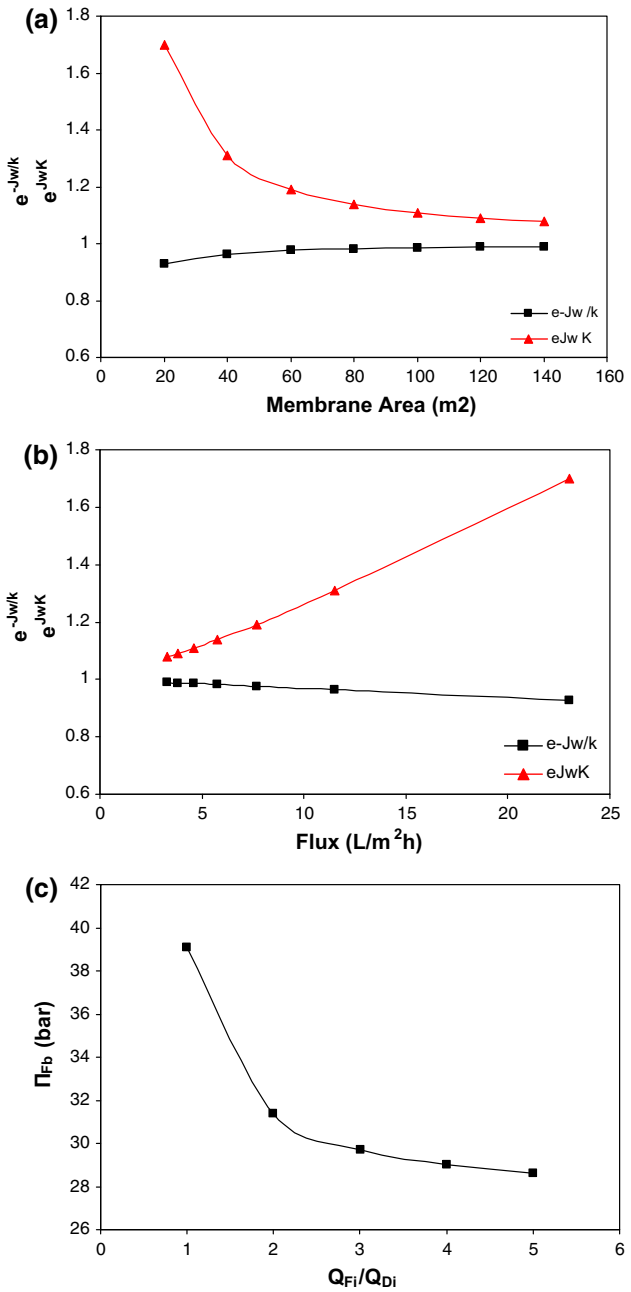

Fig. 5 Effect of membrane operating parameters on the performance of FO process. **a** Effect of membrane area on the moduli of dilutive and concentrative CP, **b** effect of permeate flux on the moduli of dilutive and concentrative CP, and **c** effect of Q_{Fi}/Q_{Di} on the osmotic pressure of bulk feed solution

were 23 and 3.3 L/m^2 h, respectively (Fig. 5a, b); the lower the J_w values, the smaller the CP effect was.

The impact of feed flow rate in terms of Q_{Fi}/Q_{Di} on the bulk osmotic pressure of feed solution, π_{Fb}, is illustrated in Fig. 5c. Initially, increasing the Q_{Fi}/Q_{Di} ratio from 1 to 2 resulted in a sharp drop of π_{Fb} and then a gradual decrease with Q_{Fi}/Q_{Di} increasing from 2 to 5. At a Q_{Fi}/Q_{Di} ratio of 1, π_{Fb} was 39 bar, but decreased to 31.4 bar at a Q_{Fi}/Q_{Di} ratio

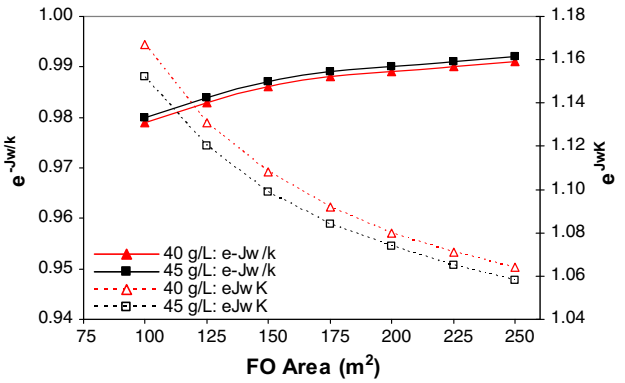

Fig. 6 Optimization FO membrane area

of 2, and reached 28.5 bar at a Q_{Fi}/Q_{Di} ratio of 5. For a given draw solution osmotic pressure, the lower the π_{Fb}, the higher the osmotic driving force across the FO membrane was. Therefore, increasing the feed flow rate was advantageous for improving the performance of the FO process and should be considered in the design parameters of the process.

Performance of optimized FO

The performance of the FO system was optimized using the method illustrated in Fig. 5. The composition of seawaters used, 35, 40, and 45 g/L, can be found in the literature (Altaee et al. 2014). NaCl was the draw solution in the FO process. The estimated permeate flow rates, Q_p, were 821, 667, and 613 m^3/h for 35, 40, and 45 g/L seawater salinity, respectively; Q_p was estimated based on the projected recovery rate of FO–RO system (Appendix 1). It should be noted that Q_p of the FO and the RO in the FO–RO system were equal.

Figure 6 shows the impact of membrane area on the modulus of dilutive and concentrative CP, $e^{\frac{-J_w}{k}}$ and $e^{J_w K}$, respectively. The values of $e^{\frac{-J_w}{k}}$ and $e^{J_w K}$ approached unity as the FO membrane area increased from 100 to 250 m^2, indicating a lower effect of CP. For example, at 45 g/L seawater salinity, $e^{\frac{-J_w}{k}}$ and $e^{J_w K}$ were 0.98 and 1.15, respectively, at 100 m^2 membrane area. However, $e^{\frac{-J_w}{k}}$ and $e^{J_w K}$ were 0.992 and 1.06, respectively, when the FO membrane area increased to 250 m^2. This latter result suggested that the impact of dilutive and concentrative CP reduced when the FO membrane area increased to 250 m^2 (Fig. 6).

The performance and operating parameters of the FO step in the FO–RO system are illustrated in Table 3. Calculations were performed to predict the feed flow rate and draw solution concentration (Appendix 1). The simulation results showed that membrane flux, J_w, decreased with increasing feed salinity. The results also showed that the

Table 3 Performance of the optimized FO process for different feed salinities

Parameter	Feed TDS 35 g/L	Feed TDS 40 g/L	Feed TDS 45 g/L
π_{Fi} (bar)	26.2	29.86	33.6
A_{FO} (m^2)	250	250	250
Q_{Di} (m^3/h)	1000	1000	1000
J_w (L/m^2 h)	3.4	2.7	2.5
C_{Di} (g/L)	65.2	66.3	71.7
π_{Di} (bar)	51.4	53.2	57.4
C_{Do} (g/L)	35.2	41	46.5
π_{Do} (bar)	28.2	31.8	35.6
Q_{Fi} (m^3/h)	2656	2294	2181
$e^{\frac{-J_w}{k}}$	0.989	0.991	0.992
$e^{J_w K}$	1.08	1.06	1.06

estimated flow rate of feed solution, Q_{Fi}, was about 2–2.5 times higher than that of the draw solution, Q_{Di}. As a matter of fact, higher feed flow rate was required at high membrane flux or permeate flow rate to reduce the bulk osmotic pressure of feed solution (Fig. 5c). Furthermore, the model predicted that the inlet concentration of the draw solution, C_{Di}, increased with increasing salinity of seawater, C_{Fi}, to maintain an adequate osmotic driving force across the FO membrane. The estimated membrane flux, J_w, was 3.3, 2.73, and 2.53 L/m^2 h for 35, 40, and 45 g/L seawater salinity, respectively. A relatively low permeation flux was required to reduce the impact of dilutive and concentrative CP, $e^{\frac{-J_w}{k}}$ and $e^{J_w K}$, respectively. Table 3 shows that the values of $e^{\frac{-J_w}{k}}$ and $e^{J_w K}$ in the optimized FO process were close to unity, which indicated an insignificant CP effect; at 35 g/L seawater salinity, for example, $e^{\frac{-J_w}{k}}$ and $e^{J_w K}$ were 0.989 and 1.08, respectively.

In general, the key parameters suggested to enhance the performance of FO process were membrane area, draw solution concentration, and feed flow rate. The effect of dilutive and concentrative CP was significantly reduced through optimizing these parameters. Furthermore, the recovery rate of RO decreased with increasing salinity of seawater in order to reduce the membrane fouling propensity (Altaee et al. 2013).

Performance of RO process

The performance of conventional RO and the RO step in the FO–RO system was evaluated for 35, 40, and 45 g/L seawater salinities. The TDS of feed water to the RO step in the FO–RO system, C_{Do}, is illustrated in Table 3. Typically, RO recovery rate was affected by the salinity of feed water. Lower RO recovery rates were applied at high seawater salinities to reduce membrane fouling; hence, at 45 g/L seawater salinity the estimated recovery rate was about 46 % and decreased to 40 and 38 % at 40 and 45 g/L seawater salinities, respectively. The feed flow rates for the conventional RO unit and the RO step in the FO–RO system were 7 and 4 m^3/h, respectively; membrane flux over time was calculated using Eq. 2 (Appendix 2). Typically, RO membrane required higher feed flow rate than the RO step in the FO–RO system because of the higher SDI of feed water. The specific energy consumption, E_s, of conventional RO and FO–RO system was calculated with and without ERD.

For a small desalination plant without ERD, the specific power consumption, E_s (kW h/m^3), for conventional RO and the RO step in the FO–RO system is shown in Fig. 7a. E_s increased with increasing age of the membrane; this was mainly attributed to the RO membrane fouling which resulted in a reduction of permeate flow. However, E_s was higher in the conventional RO unit than in the RO step in the FO–RO system because of the higher membrane fouling in the conventional RO system. The average power consumption, $E_{s\text{-ave}}$, for the conventional RO was 5.22, 6.13, and 6.97 kW h/m^3 for 35, 40, and 45 g/L seawater salinities, respectively; the corresponding $E_{s\text{-ave}}$ values for the RO step in the FO–RO step were 4.32, 4.89, and 5.8 kW h/m^3 for 35, 40, and 45 g/L seawater salinities, respectively. These results indicated that the RO step in the FO–RO system was more energy efficient than the conventional RO system when ERD was not used. This latter result was valid for seawater salinities ranging from 35 to 45 g/L.

For large desalination plants equipped with 80 % efficiency ERD, the profile of power consumption during the estimated membrane life of 5 years is illustrated in Fig. 7b. Specific power consumption, E_s, of the conventional RO unit was higher than that of the RO step in the FO–RO at seawater salinity between 35 and 45 g/L. At 35 g/L seawater salinity, E_s of the conventional RO, at year 1 and 5 of the membrane life, was 2.32 and 2.82 kW h/m^3, whereas the corresponding values for the RO step in the FO–RO system were 2.28 and 2.4 kW h/m^3, respectively. E_s

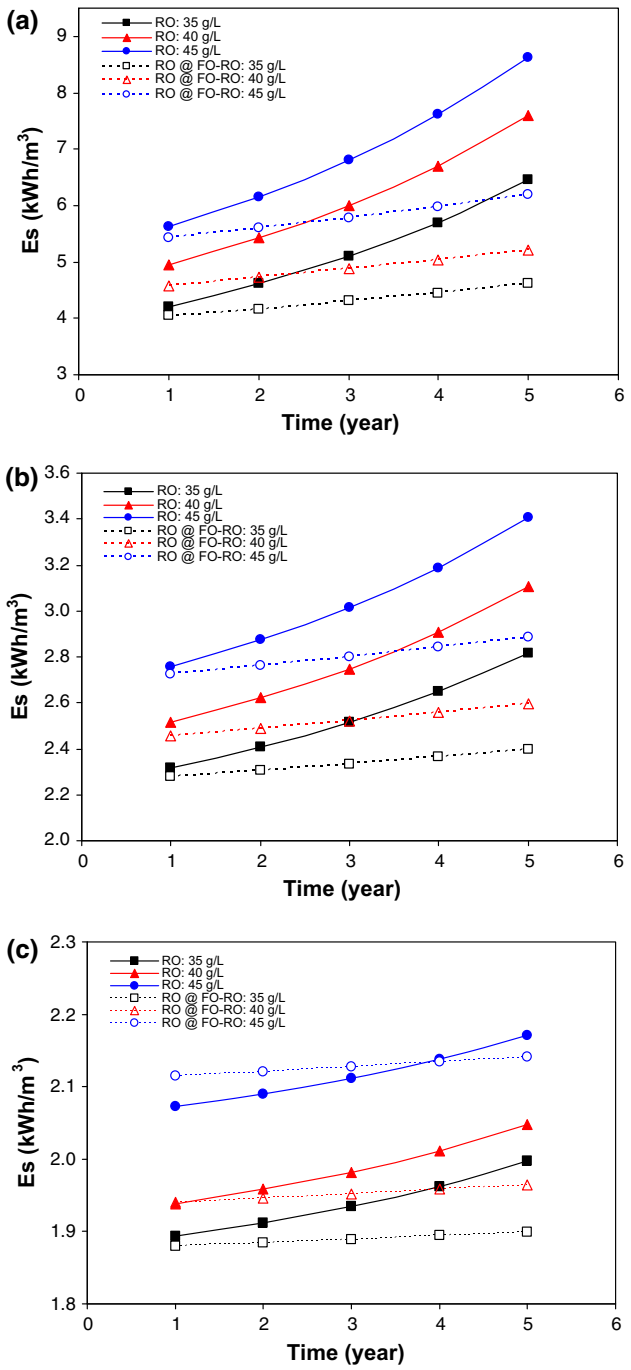

Fig. 7 Specific power consumption of conventional RO and RO step in the FO–RO. **a** Specific power consumption over time for desalination plant without ERD, **b** specific power consumption over time for desalination plant with 80 % efficiency ERD, and **c** specific power consumption for desalination plant with 98 % efficiency ERD

profiles at 40 and 45 g/L seawater salinities were similar to that at 35 g/L. The average specific power consumption, $E_{s\text{-ave}}$, was also estimated for the RO system and the RO step in the FO–RO. $E_{s\text{-ave}}$ represented the average power consumption during 5 years of the RO membrane life. For conventional RO, $E_{s\text{-ave}}$ was 2.54, 2.78, and 3.05 kW h/m^3, respectively, for 35, 40, and 45 g/L seawater salinities. The corresponding values of $E_{s\text{-ave}}$ for the RO step in the FO–RO were 2.34, 2.52, and 2.8 kW h/m^3. This result suggested that the RO step in the FO–RO system was slightly more energy efficient than a conventional RO unit at all seawater salinities under investigation, i.e. 35–45 g/L. The difference in $E_{s\text{-ave}}$ between the conventional RO unit and the RO step in the FO–RO process was about 9 % for a desalination plant with 80 % efficiency ERD, while it was about 20 % for a desalination plant without an ERD.

For conventional RO and an FO–RO system provided with an ERD of 98 % efficiency, such as pressure exchanger and turbo charger, the difference of E_s between the RO and the FO–RO becomes insignificant (Fig. 7c). At 35 and 40 g/L, E_s of the conventional RO was higher than that of the RO step in the FO–RO system during years 1–5 of the membrane life. On the contrary, at 45 g/L seawater salinity, E_s of the RO was lower than that of the RO step in the FO–RO during years 1–4 of the membrane life but slightly increased at year 5 of the membrane life. On the other hand, $E_{s\text{-ave}}$ for conventional RO was 1.94, 1.99, and 2.12 kW h/m^3, respectively, for 35, 40, and 45 g/L seawater salinities. The corresponding values of $E_{s\text{-ave}}$ for FO–RO were 1.89, 1.95, and 2.13 kW h/m^3. The results indicated that energy efficiency difference between the conventional RO unit and the FO–RO system decreased with a 98 % efficiency ERD system.

For desalination plants without ERD, there was a slightly tangible difference of $E_{s\text{-ave}}$ between conventional RO and FO–RO. However, for a desalination plant with ERD system, the difference of power consumption between the conventional RO and the FO–RO was small enough for the FO and pretreatment power consumptions to have a significant impact on the system's overall power consumption. Therefore, we have included them in a second approximation.

Table 4 shows the total average specific power consumption, $E_{s\text{-ave-tot}}$, in the conventional RO and FO–RO processes for 35, 40, and 45 g/L seawater concentrations (Gude 2011). $E_{s\text{-ave-tot}}$ was calculated for 80 and 98 % ERD efficiency. In addition to the power consumption in the RO process, E_s for pumping seawater in intake system, pretreatment, and FO pretreatment (if applicable) was included in the $E_{s\text{-ave-tot}}$. The average specific power consumption was calculated from Eq. 4 using the average permeate flow. It was assumed that feed pressure of the feed and the draw solutions in the FO process was 1 bar. Statistically, for the FO–RO process, 80 % of the $E_{s\text{-ave-tot}}$ was due to the RO process and about 15 % was due to the seawater pretreatment, whereas the contribution of the FO process was only 5 % of the total average power consumption. The breakdown of $E_{s\text{-ave-tot}}$ for the conventional

Table 4 Total average specific power consumption, $E_{s\text{-ave-tot}}$, in the RO and FO–RO; $E_{s\text{-ave-tot}}$ only includes pumping seawater from the intake system and pretreatment, pump efficiency is 0.8, and feed flow rate is 7 and 4 m^3/h for the RO and the FO–RO, respectively

System	SW (mg/L)	Process	P (bar)	Power (kW h)	$Q_{p\text{-ave}}$ (m^3/h)	$E_{s\text{-ave-p}}$ (kW h/m^3)	$E_{s\text{-ave-FO}}$ (kW h/m^3)	$E_{s\text{-ave-RO}}$ (kW h/m^3)	$E_{s\text{-ave-tot}}$ (kW h/m^3)
RO	35	Intake-S	4	0.97	2.44	0.40	–	2.54[a]	3.14[a]
		Pret-S	2	0.49	2.44	0.20		1.94[b]	2.54[b]
	40	Intake	4	0.97	2.12	0.46	–	2.78[a]	3.47[a]
		Pretreat.	2	0.49	2.12	0.23		1.99[b]	2.68[b]
	45	Intake	4	0.97	2.02	0.48	–	3.05[a]	3.77[a]
		Pretreat.	2	0.49	2.02	0.24		2.12[b]	2.84[b]
FO–RO	35	Intake	4	0.56	1.67	0.33	0.14	2.34[a]	2.98[a]
		Pretreat.	2	0.28	1.67	0.17		1.89[b]	2.53[b]
	40	Intake	4	0.56	1.45	0.38	0.16	2.52[a]	3.09[a]
		Pretreat.	2	0.28	1.45	0.19		1.95[b]	2.68[b]
	45	Intake	4	0.56	1.38	0.40	0.17	2.80[a]	3.4[a]
		Pretreat.	2	0.28	1.38	0.20		2.13[b]	2.95[b]

Intake-S intake system, *Pret-S* pretreatment system, $Q_{p\text{-ave}}$ average permeate flow over 5 years, $E_{s\text{-ave-p}}$ average initial power consumption in intake system or pretreatment, $E_{s\text{-ave-FO}}$ average power consumption in FO, $E_{s\text{-ave-RO}}$ average power consumption in RO, $E_{s\text{-ave-tot}}$ average total power consumption in system (RO or FO–RO)

[a] ERD efficiency 80 %

[b] ERD efficiency 90 %

Table 5 Membrane area and number of elements required for 20,000 m^3/day desalination plant

Seawater TDS (mg/L)	FO–RO system				Conventional RO system	
	FO		RO			
	A_{FO} (m^2)	No. elem.	A_{RO} (m^2)	No. elem.	A_{RO} (m^2)	No. elem.
35	470,491	1882	148,017	3700	101,256	2531
40	520,183	2081	170,068	4252	116,387	2910
45	548,607	2194	179,211	4480	122,549	3064

RO was 20 and 80 % for the pretreatment stage and RO process, respectively. For a desalination plant with 80 % ERD efficiency, results showed that $E_{s\text{-ave-tot}}$ in the FO–RO system was 5–10 % lower than that in the conventional RO process. For a desalination plant with 98 % ERD efficiency, $E_{s\text{-ave-tot}}$ in the conventional RO was equal to that in the FO–RO system at 35 and 40 g/L feeds. At 45 g/L seawater salinity, $E_{s\text{-ave-tot}}$ was lower in the conventional RO unit than in the FO–RO system. The results disagreed with previous findings which suggested that an FO–RO system could be more energy efficient at high seawater salinities. Using a high-efficiency ERD system not only reduced the cost of the RO process but became more competitive to the FO–RO even at high feed salinities. Therefore, the application of FO–RO should be limited to small desalination plants without ERD systems or feed waters with high fouling materials.

Membrane requirement

Membrane requirements in the conventional RO unit and FO–RO system were different. Membrane area was calculated for a 20,000 m^3/day conventional RO and FO–RO desalination plants. Three feed water salinities, 35, 40, and 45 g/L, were evaluated. It was assumed here that FO membrane area, A_{FO}, was about 250 m^2. In general, the estimated membrane area was higher at higher seawater salinities (Table 5); this holds for both the conventional RO and the FO–RO system and it was attributed to the lower membrane flux at higher seawater salinity. A_{FO} was higher than the RO membrane area, A_{RO}, because of the lower membrane flux in the FO process; this was essential in the design model to reduce the effect of CP. It should be mentioned that the membrane life in the FO–RO system was likely to exceed 5 years because of the lower degree of

fouling, while membrane life in the conventional RO system was expected to be around 5 years.

Conclusions

Several previous studies examined the potential of using FO–RO systems for seawater desalination, and concluded that one distinct disadvantage of the FO–RO process was the greater energy consumption. Therefore, FO–RO was only recommended for the desalination of high-salinity seawaters where conventional RO was less efficient. The current study evaluated the efficiency of an FO–RO system, at feed salinities between 35 and 45 g/L, in comparison with a conventional RO unit taking into account annual flux decline due to membrane fouling. For a small RO desalination plant without ERD, $E_{\text{s-ave-tot}}$ was between 5.22 and 6.97 kW h/m^3. For the same operating conditions, the $E_{\text{s-ave-tot}}$ of FO–RO system was between 4.32 and 5.80 kW h/m^3, indicating that FO–RO system was more energy efficient. When 98 % efficiency ERD was employed, results showed that $E_{\text{s-ave-tot}}$ was between 2.54 and 2.84 kW h/m^3 for the conventional RO unit, whereas for the FO–RO system it was between 2.53 and 2.95 kW h/m^3. This suggested that the conventional RO process was more efficient than an FO–RO system, especially when a high-efficiency ERD was employed. Furthermore, an FO–RO system required twice the membrane area required compared to a conventional RO unit which would further compromise the cost of desalinated water. For a desalination plant without an ERD, an FO–RO system was relatively more energy efficient than conventional RO. These results have a strong significance for decision making in desalination implementation when there are high salinity and a limitation of energy. In general, the results suggest that FO–RO system was less energy efficient than a conventional RO unit regardless of the feed salinity, but this latter approach could be considered for small desalination plants without an ERD system. However, long-term pilot plant tests are suggested to be conducted in order to support the conclusions of this study.

Appendix 1: Optimization of FO performance

FO optimization was performed to reduce the energy requirements of the FO–RO system. Calculation was carried out at 35 g/L seawater salinity and 46 % recovery rate using NaCl draw solution. We assumed that Q_{p} was equal in both the FO and RO membranes and Q_{Di} was 1000 L/h (Table 3); permeate flow rate of the RO step in the FO–RO system was given as

$$\%\text{Re} = 0.46 = \frac{Q_{\text{p}}}{Q_{\text{Di}} + Q_{\text{p}}} = \frac{Q_p}{1000\,\text{L/h} + Q_{\text{p}}}$$
$$Q_{\text{p}} = 851\,\text{L/h}.$$

Membrane flux, J_{w}, was calculated from the following equation assuming that FO membrane area was 250 m^2 (Table 3):

$$J_{\text{w}} = \frac{851\,\text{L/h}}{250\,\text{m}^2} = 3.4\,\text{L/m}^2\,\text{h}.$$

The permeate TDS was calculated from Eq. 22 and using B value from Table 1 as follows:

$$C_{\text{p}} = \frac{0.12\,\text{kg/m}^2\,\text{h} \times 35000\,\text{mg/kg}}{0.34\,\text{L/m}^2\,\text{h} + 0.12\,\text{kg/m}^2\,\text{h}} = 1208\,\text{mg/kg}.$$

The outlet concentration of Na, C_{Nao}, was calculated from Eq. 18; $\pi_{\text{Do}}(\pi_{\text{Do}} = \pi_{\text{Fi}} + 2)$ was 28.2 bar (Table 3) and $C_{\text{Clo}} = 1.54 \times C_{\text{Nao}}$:

$$\pi_{\text{Do}} = \frac{C_{\text{Nao}} \times 1.12 \times T}{M_{\text{Na}} \times 14.5} + \frac{\left(\frac{M_{\text{Cl}}}{M_{\text{Na}}}\right) \times C_{\text{Nao}} \times 1.12 \times T}{M_{\text{Cl}} \times 14.5}$$
$$28.2\,\text{bar} = \frac{C_{\text{Nao}} \times 1.12 \times (273 + 30)}{23 \times 10^3 \times 14.5} + \frac{1.54 \times C_{\text{Nao}} \times 1.12 \times (273 + 30)}{35.45 \times 10^3 \times 14.5}$$
$$C_{\text{Nao}} = 13864\,\text{mg/L}.$$

The outlet concentration of Cl, C_{Clo}, was calculated from the following equation:

$$C_{\text{Clo}} = 1.54 \times 13864 = 21369\,\text{mg/L}.$$

The outlet concentration of NaCl draw solution is 35,233 mg/L. Inlet concentration of the draw solution was calculated from mass balance (Fig. 3) using Eq. 21:

$$C_{\text{Di}} = \frac{(C_{\text{Do}} \times Q_{\text{Do}}) - (Q_{\text{p}} \times C_{\text{p}})}{Q_{\text{Di}}} = \frac{(1851 \times 35234) - (851 \times 1208)}{1000} = 64190\,\text{mg/L}.$$

The inlet concentrations of Na^+ and Cl^-, C_{Nai} and C_{Cli}, respectively, were

$$C_{\text{Nai}} = 64190 \times \frac{23}{58.45} = 25259\,\text{mg/L}$$
$$C_{\text{Cli}} = 64190 \times \frac{35.45}{58.45} = 38931\,\text{mg/L}.$$

The inlet osmotic pressure of draw solution, π_{Di}, was calculated from C_{Nai} and C_{Cli} as follows:

$$\pi_{\text{Di}} = \frac{25663 \times 1.12 \times (273 + 30)}{23 \times 10^3 \times 14.5} + \frac{38931 \times 1.12 \times (273 + 30)}{35.45 \times 10^3 \times 14.5} = 51.4\,\text{bar}.$$

The bulk osmotic pressure of draw solution, π_{Db}, was $(51.4 + 28.2)/2 = 39.8$ bar. The bulk osmotic pressure of the feed solution, π_{Fb}, was calculated from Eq. 23 as follows:

$$\pi_{Fb} = \frac{\pi_{Db} \times e^{\frac{-J_w}{k}} - \left[\left(1 + \frac{B}{J_w}\left(e^{J_w K} - e^{\frac{-J_w}{k}}\right)\right) \times \frac{J_w}{A_w}\right]}{e^{J_w K}}$$

$$\pi_{Fb} = \frac{39.8 \times 0.989 - \left[\left(1 + \left(\frac{0.12}{3.4}\right) \times (1.08 - 0.989)\right) \times \frac{3.4}{0.79}\right]}{1.08}$$

$$= 32.4\,\text{bar}.$$

The outlet osmotic pressure of feed solution, π_{Fo}, was calculated from Eq. 24:

$$\pi_{Fo} = \pi_{Fb} \times 2 - \pi_{Fi} = (32.4 \times 2) - 26.2 = 38.6\,\text{bar}.$$

FO recovery rate was calculated from Eq. 27 as follows:

$$\text{Re} = 1 - \frac{\pi_{Fi}}{\pi_{Fo}} = 1 - \frac{26.2}{38.6} = 0.32\,\%.$$

The feed flow rate was calculated from Eq. 28:

$$Q_{Fi} = \frac{Q_p}{\text{Re}} = \frac{851}{0.32} = 2656\,\text{L/h}.$$

Appendix 2: Water flux decline in RO

Annual decline in membrane flux was calculated from Eq. 2, assuming 8 and 3 % annual flux decline in the conventional RO and the RO step in the FO–RO system, respectively. For the FO–RO system operating at 46 % recovery rate and 3 % annual flux decline, the initial water flux was 6.19 L/m^2 h. Water flux in year 1 was calculated as follows (Fig. 8):

$$J_n = J_o - (Y_n \cdot J_0) = 6.19 - (6.19 \times 0.3) = 6\,\text{L/m}^2\text{h}.$$

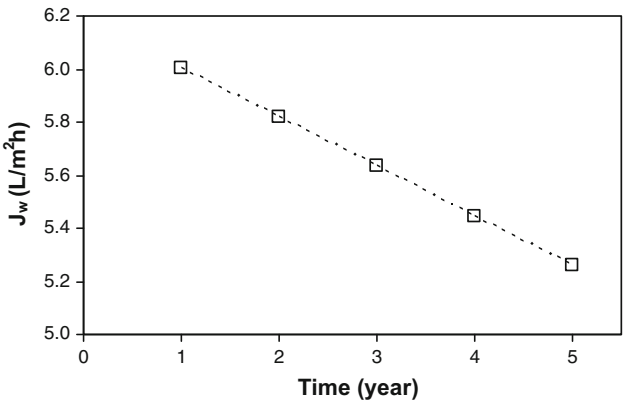

Fig. 8 Membrane flux in the RO step in the FO–RO system at 35 g/L feed salinity

References

Achilli A, Cath TY, Childress AE (2009) Power generation with pressure retarded osmosis: an experimental and theoretical investigation. J Membr Sci 343:42–52

Al-Mutaz IS, Wazeer I (2015) Current status and future directions of MED-TVC desalination technology. Desalin Water Treat 55:1–9

AlTaee A, Sharif AO (2011) Alternative design to dual stage NF seawater desalination using high rejection brackish water membranes. Desalination 273:391–397

Altaee A, Zaragoza G (2014) A conceptual design of low fouling and high recovery FO-MSF desalination plant. Desalination 343:2–7

Altaee A, Mabrouk A, Bourouni K (2013) A novel forward osmosis membrane pretreatment of seawater for thermal desalination processes. Desalination 326:19–29

Altaee A, Zaragoza G, van Tonningen HR (2014) Comparison between forward osmosis–reverse osmosis and reverse osmosis processes for seawater desalination. Desalination 336:50–57

Bataineh KM (2016) Multi-effect desalination plant combined with thermal compressor driven by steam generated by solar energy. Desalination 385:39–52

Bates W, Bartels C, Polonio L (2015) Improvements in RO technology for difficult feed waters. Hydranautics Nito Dinko. http://www.membranes.com/docs/papers/New%20Folder/Improvements%20in%20RO%20Technology%20for%20Difficult%20Feed%20Waters%20final%20020311.pdf

Bennett A (2015) Developments in desalination and water reuse. Filtr Sep 52:28–33

Bhinder A, Fleck BA, Pernitsky D, Sadrzadeh M (2016) Forward osmosis for treatment of oil sands produced water: systematic study of influential parameters. Desalin Water Treat. doi:10.1080/19443994.2015.1108427

Chekli L, Phuntsho S, Kim JE, Kim J, Choi JY, Choi J-S, Kim S, Kim JH, Hong S, Sohn J, Shon HK (2016) A comprehensive review of hybrid forward osmosis systems: performance, applications and future prospects. J Membr Sci 497:430–449

Chung T-S, Luo L, Wan CF, Cui Y, Amy G (2015) What is next for forward osmosis (FO) and pressure retarded osmosis (PRO). Sep Purif Technol 156(2):856–860

Cipollina A, Tzen E, Subiela V, Papapetrou M, Koschikowski J, Schwantes R, Wieghaus M, Zaragoza G (2015) Renewable energy desalination: performance analysis and operating data of existing RES-desalination plants. Desalin Water Treat 55(11):3120–3140

Dimitriou E, Mohamed ES, Karavas C, Papadakis G (2015) Experimental comparison of the performance of two reverse osmosis desalination units equipped with different energy recovery devices. Desalin Water Treat 55:3019–3026

Gilron J (2014) Water-energy nexus: matching sources and uses. Clean Technol Environ Policy 16(8):1471–1479

Gude VG (2011) Energy consumption and recovery in reverse osmosis. Desalin Water Treat 36:239–260

Gude VG (2016) Desalination and sustainability—an appraisal and current perspective. Water Res 89:87–106

Hoang M, Bolto B, Haskard C, Barron O, Gray S, Leslie G (2009) Desalination plants: an australia survey. Water 36:67–73

Horta P, Zaragoza G, Alarcón-Padilla DC (2015) Assessment of the use of solar thermal collectors for desalination. Desalin Water Treat 55(10):2856–2867

Hydranautics Design Limits (2015) Hydranautics Nito Dinko. www.membranes.com/docs/trc/Dsgn_Lmt.pdf

Iwahori H, Ando M, Nakahara R, Furuichi M, Tawata S, Yamazato T (2003) Seven years operation and environmental aspects of 40,000 m^3/d seawater RO plant at Okinawa, Japan. In: Proceedings of the IDA congress, Bahamas

Jiang Y (2015) China's water security: current status, emerging challenges and future prospects. Environ Sci Policy 54:106–125

Kim SJ, Oh BS, Yu HW, Kim LH, Kim CM, Yang ET, Shin MS, Jang A, Hwang MH, Kim IS (2015) Foulant characterization and distribution in spiral wound reverse osmosis membranes from different pressure vessels. Desalination 370:44–52

Luo H, Wang Q, Zhang TC, Tao T, Zhou A, Chen L, Bie X (2014) A review on the recovery methods of draw solutes in forward osmosis. J Water Process Eng 4:212–223

Majeed T, Sahebi S, Lotfi F, Kim JE, Phuntsho S, Tijing LD, Shon HK (2015) Fertilizer-drawn forward osmosis for irrigation of tomatoes. Desalin Water Treat 53(10):2746–2759

Mamo J, Pikalov V, Arrieta S, Jones AT (2013) Independent testing of commercially available, high-permeability SWRO membranes for reduced total water cost. Desalin Water Treat 51:184–191

Maxwell S (2010) A look at the challenges—and opportunities—in the world water market. J Am Water Works Assoc 102:104–116

Mazlan NM, Peshev D, Livingston AG (2016) Energy consumption for desalination—a comparison of forward osmosis with reverse osmosis, and the potential for perfect membranes. Desalination 377:138–151

McGovern RK, Lienhard JHV (2014) On the potential of forward osmosis to energetically outperform reverse osmosis desalination. J Membr Sci 469:245–250

Mezher T, Fath H, Abbas Z, Khaled A (2011) Techno-economic assessment and environmental impacts of desalination technologies. Desalination 266:263–273

Nasr P, Sewilam H (2015) Forward osmosis: an alternative sustainable technology and potential applications in water industry. Clean Technol Environ Policy V17:2079–2090

Patroklou G, Mujtaba MI (2014) Economic optimisation of seawater reverse osmosis desalination with boron rejection. Comput Aided Chem Eng V33:1381–1386

Peñate B, García-Rodríguez L (2011) Energy optimisation of existing SWRO (seawater reverse osmosis) plants with ERT (energy recovery turbines): technical and thermoeconomic assessment. Energy 36:613–626

Qin JJ, Liberman B, Kekre KA (2009) Direct osmosis for reverse osmosis fouling control: principles, applications and recent developments. Open Chem Eng J 3:8–16

Rachman RM, Ghaffour N, Wali F, Amy GL (2013) Assessment of silt density index (SDI) as fouling propensity parameter in reverse osmosis (RO) desalination systems. Desalin Water Treat 51:1091–1103

Rodríguez-Calvo A, Silva-Castro GA, Osorio F, González-López J, Calvo C (2015) Reverse osmosis seawater desalination: current status of membrane systems. Desalin Water Treat 56(4):849–861

Roy D, Rahni M, Pierre P, Yargeau V (2016) Forward osmosis for the concentration and reuse of process saline wastewater. Chem Eng J 287:277–284

Salgot M (2008) Water reclamation, recycling and reuse: implementation issues. Desalination 218:190–197

Sato Y, Nakao S-I (2016) Theoretical estimation of semi-permeable membranes leading to development of forward osmosis membranes and processes as a future seawater desalination technology. Desalin Water Treat 57(12):5398–5405

Shaffer DL, Werber JR, Jaramillo H, Lin S, Elimelech M (2015) Forward osmosis: where are we now? Desalination 356:271–284

Stover RL (2007) Seawater reverse osmosis with isobaric energy recovery devices. Desalination 203:168–175

Su J, Zhang S, Ling MM, Chung T-S (2012) Forward osmosis: an emerging technology for sustainable supply of clean water. Clean Technol Environ Policy 14(4):507–511

Sun C, Xie L, Li X, Sun L, Dai H (2015) Study on different ultrafiltration-based hybrid pretreatment systems for reverse osmosis desalination. Desalination 371:18–25

Tiraferri A, Yip NY, Straub AP, Castrillon Romero-Vargas S, Elimelech M (2013) A method for the simultaneous determination of transport and structural parameters of forward osmosis membranes. J Membr Sci 444:523–538

Valladares RL, Li Z, Sarp S, Bucs SS, Amy G, Vrouwenvelder JS (2014) Forward osmosis niches in seawater desalination and wastewater reuse. Water Res 66:122–139

Webley J (2015) Technology developments in forward osmosis to address water purification. Desalin Water Treat 55:2612–2617

Youssef PG, Al-Dadah RK, Mahmoud SM (2014) Comparative analysis of desalination technologies. Energy Procedia 61: 2604–2607

Zhao D, Chen S, Guo CX, Zhao Q, Lu X (2016) Multi-functional forward osmosis draw solutes for seawater desalination. Chin J Chem Eng 24(1):23–30